Outage Probability for Diversity Combining in Interference-Limited Channels

Aditya Chopra, *Student Member, IEEE,* and Brian L. Evans, *Fellow, IEEE*

Abstract

Many wireless data communication systems such as LTE, and Wi-Fi, are increasingly facing interference that is much stronger than thermal noise. Interference may arise due to dense spatial reuse of spectrum intended to increase user data rates, or from other devices emitting radiation in the same spectrum, or from electronic circuitry within the communication platform. For a multi-antenna receiver operating in an interference-limited channel, we evaluate four diversity combining algorithms in terms of outage probability in the low-outage regime. The contributions of this paper are (1) derivation of closed-form expressions for the output signal-to-interference ratio (SIR) statistics of fixed weight, maximal ratio, selection and post-detection combining; (2) comparison of the relative outage performance of these algorithms; and (3) proposed diversity combining algorithms to reduce outage probability. Our results can be applied in analyzing the outage performance and throughput capacity of both centralized and decentralized interference-limited wireless networks.

Index Terms

Co-channel interference, symmetric alpha stable, Poisson point processes, impulsive noise, diversity reception, outage probability, spatial dependence.

Submitted on September 14, 2011. A. Chopra and B. L. Evans are with the Wireless Networking and Communications Group, Department of Electrical and Computer Engineering, The University of Texas at Austin, TX 78712 USA e-mail: achopra@utexas.edu, bevans@ece.utexas.edu.

This research was supported by Intel Corporation.

I. Introduction

Wireless transceivers suffer degradation in communication performance due to interference generated by both human-made and natural sources [1]. Human-made sources of interference include uncoordinated wireless devices operating in the same frequency band (co-channel interference) [2], devices communicating in adjacent frequency bands (adjacent channel interference), and computational platform subsystems radiating clock frequencies and their harmonics [3]. Dense spatial reuse of the available radio spectrum, which is key in meeting increasing demand in user data rates [4], also causes severe co-channel interference and may limit communication system performance.

Recent communication standards and research have focused on the use of multiple receive antennas to increase data rate and communication reliability in wireless networks. Single input multiple output (SIMO) communication systems can achieve higher data rates with fewer errors through *spatial diversity*; i.e., receiving multiple copies of the signal increases the chance that some of these copies are relatively impairment free. Consequently, wireless receivers with multiple antennas are increasingly being deployed in network environments that are rife with interference due to resource reuse [1], [2]. Multi-antenna wireless receivers have generally been designed and their communication performance analyzed under the assumption of additive Gaussian noise. While the Gaussian distribution is a good statistical model for thermal noise at the receiver, interference has predominantly non-Gaussian statistics. This mismatch between design assumptions and the actual interference statistics may degrade the communication performance of multi-antenna wireless receivers. Since communication systems utilizing multiple antennas are being deployed on mobile platforms, it becomes essential to characterize the relative performance of spatial diversity techniques in the presence of interference.

In this paper, we analyze the performance of diversity combining techniques in interference-limited channels; i.e., we assume that the non-Gaussian interference is significantly stronger than Gaussian noise at the receiver. Interference is modeled via statistical-physical mechanisms of interferer distribution, interference generation, and interference propagation. The diversity combining receivers under study are the equal gain combiner (EGC), fixed weight

combiner (FWC), maximum ratio combiner (MRC), selection combiner (SC), and the post-detection combiner (PDC). A detailed discussion on each of these receivers can be found in Sections IV and V. Evaluating the performance of these diversity combining algorithms in interference highlights the relative merits or disadvantages of different algorithms in different interference environments. We also propose a novel diversity combining algorithm that improves upon the performance of current diversity combining receivers.

A. Organization

In Section II we discuss the key contributions and limitations of prior work on communication performance in interference limited systems. Section III details our system model for interferer location distribution, and interference generation and propagation. In Section IV we derive the outage probability of pre-detection diversity combining techniques. We derive closed-form outage probability expressions for fixed weight combining, maximum ratio combining and selection combining. In Section V we derive the outage probability expression for a post detection combining receiver. Section VI presents numerical simulations to compare our closed-form outage probability to simulated outage in a multi-antenna receiver located within a space containing Poisson distributed interferers. In Section VII, two novel diversity combining receivers are proposed and their communication performance is compared to existing algorithms studied in Sections IV and V. We conclude with a summary of the key contributions and insights in Section VIII.

B. Notation

Scalar random variables are represented using lower-case notation, random vectors are denoted using the boldface lower-case notation, and random matrices are denoted using the boldface upper-case notation. Deterministic parameters are represented using Greek alphabet, with the exception of N denoting the number of receive antennas. $\mathbb{E}_x\left\{f(x)\right\}$ denotes the expectation of the function $f(x)$ with respect to the random variable x, $\mathbb{P}(\cdot)$ denotes the probability of a random event, $\|\cdot\|$ denotes the vector 2−norm, and $\|\cdot\|_p$ denotes

the vector $p-$norm. $\binom{N}{m}$ denotes the number of possible ways of choosing m objects out of a total of n, which is equal to $\frac{n!}{(n-m)!m!}$.

II. Prior Work

Prior work on analyzing communication performance of receiver diversity algorithms in interference has often focused on bit-error rate (BER) analysis of various reception schemes in the presence of additive impulsive noise. Typical statistical distributions that model impulsive noise are the spherically invariant symmetric alpha-stable distribution [5], spherically invariant Middleton Class A distribution [6], and multi-dimensional independent Middleton Class A noise model [6]. These statistical distributions model two extreme cases of interference statistics; i.e, interference is either statistically isotropic across antennas or statistically independent across receive antennas.

In [7], the isotropic symmetric alpha-stable noise model was used to evaluate BER under various diversity combining schemes. This work was extended in [8] to more reception techniques, but only considered Binary Phase Shift Keying (BPSK) modulation. In [9], the authors investigated the performance of different diversity combining techniques over fading channels with impulsive noise modeled using either isotropic or independent multi-dimensional Middleton Class A distribution. In [10], the authors analyze performance bounds for optimum and sub-optimum receivers in the presence of Middleton Class A impulsive noise over non-fading channels. In [11], the authors evaluate performance bounds of 2×2 MIMO communication with Alamouti codes using a generalized statistical-physical interference model from [12]. In [13] the performance of maximum ratio combining techniques was investigated in multi-user environments and in presence of receiver channel estimation error. While the authors did use the notion of statistical-physical interference propagation mechanisms, they assumed a fixed number and locations of the interference generating sources. In [14], a statistical-physical model similar to ours was used to study performance of optimum diversity combining. However, this model also assumed that interference was isotropic and the optimum receiver was impractical to implement as it required information about interferer locations at each sampling instant.

TABLE I
PRIOR WORK ON ANALYSIS OF RECEIVE DIVERSITY PERFORMANCE IN A POISSON FIELD OF INTERFERERS. CONTINUUM REFERS TO A CONTINUUM BETWEEN ISOTROPIC AND INDEPENDENT. (SAS: SYMMETRIC ALPHA STABLE, MCA: MIDDLETON CLASS A)

	Interference Model				Diversity Combiner				
Paper	Type	Isotropic	Independent	Continuum	FWC	MRC	SC	PDC	MMSE
[8]	SAS	✓			✓	✓	✓	✓	
[9]	MCA	✓	✓		✓	✓	✓	✓	
[13]	SAS	✓	✓			✓			
[14]	SAS	✓	✓						✓
this	SAS	✓	✓	✓	✓	✓	✓	✓	

Table I summarizes interference models and receiver algorithms in [8], [9], [13], [14] and in this paper. By using impulsive statistical distributions to model interference, performance analysis in [8], [9], [13] provides a link between communication performance and noise parameters. On the other hand, by starting from a statistical-physical interference generation mechanism, performance analysis in [14] provides a link between communication performance and network parameters such as user density and user distribution.

III. SYSTEM MODEL

A. Network Model

In this section, we describe a interference limited multi-antenna wireless communication system via the following assumptions:

I) The communication link comprises of one transmit antenna and N receive antennas.

II) Interferers are located in a two-dimensional plane around the receiver. This assumption is used only for ease of analysis. Distributing interferers in a three-dimensional volume does not alter the nature of any of our results, other than certain parameter values.

III) At each time snapshot, the active interfering sources are classified into $N+1$ independent sets $\mathscr{S}_0, \mathscr{S}_1, \cdots, \mathscr{S}_N$. $\mathscr{S}_0$ denotes the set of interferers that cause interference to every receive antenna. $\mathscr{S}_n \ \forall \ n = 1, \cdots, N$ denotes the set of interferers that are observed by antenna n alone. This is the key assumption in our framework for modeling spatial dependence in interference observed by a multi-antenna receiver. In prior work, interference is often modeled as being one of two extremes; i.e, either all interferers

are observed by every receive antenna, or different receivers observe independent sets of interferers. Our model generalizes this notion, ensuring that our results are not only applicable to these two extreme scenarios, but also to a continuum between these two extremes. A common scenario in which such an interferer environment may arise is with the deployment of receivers employing sectorized antennas with full frequency reuse. Sectorized antennas are geographically co-located wireless directional antennas with radiation patterns shaped as partially overlapping sectors that combine to cover the entire space around the multi-antenna system [15]. Combining the signals received by sectorized antennas can provide the advantages of spatial diversity while mitigating the impairments caused by multipath delay [16]. Interference signals common to all antennas may arise in overlapping sections; i.e., where all antennas have similar antenna gain, and individual antennas may still see independent interference in sectors where one antenna exhibits high gain while others exhibit a null. This model also finds use in multi-dimensional temporal [17] and spatial interference modeling [18].

IV) At each sampling time instant, the locations of the active interferers in $\mathscr{S}_n \ \forall \ n=0,\cdots,N$ are distributed according to a homogeneous spatial Poisson Point Process in the two-dimensional plane around the receiver. The intensity of set $\mathscr{S}_n$ is denoted by $\lambda_n \ \forall \ n=0,\ldots,N$. The Poisson Point Process distribution is usually applied to modeling the statistical distribution of interfering sources in wireless communication systems [19]. While non-homogeneous Poisson Point Processes are also used to model certain wireless networks [20], this paper only studies networks where interfering sources are modeled as homogeneous Point Processes. A spatial Poisson point process distribution of interferers allows each interferer set $\mathscr{S}_n$ to have potentially infinite number of interferers. The distance of each interferer from the origin provides an ordering function, ensuring that the interferers in each set are countable. In other words, the i^{th} interferer in $\mathscr{S}_n$, located at coordinates $\mathbf{R}_{n,i}$, is defined by implicitly assuming $\|\mathbf{R}_{n,1}\|_2 < \|\mathbf{R}_{n,2}\|_2 < \|\mathbf{R}_{n,3}\|_2 < \cdots$.

V) There are no interferer-free *guard-zones* around the receiver. In many centralized communication systems, a central authority such as a base station may limit transmissions

within a radius around an active receiver. Many medium access control protocols can also enforce such a *guard-zone* around the receiver [21], [22]. There are well known statistical distributions that model multi-antenna interference in the presence of interferer free *guard-zones* around the receiver [20], [23], and there exists prior work on evaluating communication performance of diversity combining techniques using such statistical models [9]. However, the absence of guard-zones is vital to modeling interference in decentralized *ad hoc* networks, as well as interference from uncoordinated users in centralized networks [24].

VI) As the wireless signal traverses through the environment, its energy decays according to the power-law path-loss model [25] with a coefficient of γ.

VII) The fast-fading channel between the transmitting source and receiver, as well as other interfering sources and the receiver is modeled using a Rayleigh distribution [25].

VIII) Additive thermal noise is ignored at the receiver. With high user density and frequency reuse, many communication systems are interference-limited; i.e., interference at the receiver is much stronger than the thermal noise component. Consequently, our results are applicable to interference-limited communication scenarios.

IX) Without loss of generality and to simplify derivations, the receiver is placed at the origin of the two-dimensional plane. Since the spatial Poisson Point Process is invariant to translation [26], any derived results remain unchanged by our choice of origin.

Figure 1 illustrates the interferer placement model for a 3-antenna receiver. In this framework, each receive antenna n observes a Poisson distributed interferer field which is the union of interferer sets $\mathscr{S}_0$ and $\mathscr{S}_n$. The common set of interferers in $\mathscr{S}_0$ models correlation between the interferer fields of two antennas. The level of correlation can be tuned by changing the intensity of $\mathscr{S}_0$ relative to the intensities of the other sets, yielding the following three interference generation scenarios:

Spatially independent interference - Interferer set $\mathscr{S}_0$ is empty, i.e., $\lambda_n>0$ and $\lambda_0=0$. In this scenario, each receiver is under the influence of an independent set of interferers. The resulting interference also exhibits independence across the receive antennas.

Spatially isotropic interference - Interferer sets $\mathscr{S}_n \ \forall \ n=1,\cdots,N$ are empty sets, i.e., λ_n=0 and λ_0>0. All receivers observe the same set of interferers, thereby causing the resulting interference to have spatial dependence across receive antennas. It has been shown that the resulting interference follows the isotropic multi-dimensional symmetric alpha-stable distribution [5].

Spatially dependent interference - All interferer sets are non-empty, i.e., λ_n>0 and λ_0>0. This models partial correlation in the interferer field observed by each of the receive antennas. The resulting interference exhibits spatial dependence across receive antennas.

B. Signal and interference representation

The received signal in a $1\times N$ SIMO communication system can be denoted in vector form as

$$\mathbf{y}=\mathbf{h}s+\mathbf{z} \tag{1}$$

where $\mathbf{y}$ is a complex $1\times N$ vector where each element y_n denotes the received signal at n^{th} of the N receive antennas. The n^{th} receive antenna observes the transmitted signal s after it has encountered a Rayleigh fading medium h_n and additive interference z_n. In (1), random variables h_n and z_n are stacked to form $1\times N$ vectors $\mathbf{h}$ and $\mathbf{z}$, respectively.

In Section III, we classified interfering sources into different sets, such that the n^{th} receive antenna observes interference from two sets that contain (1) interferers observed by all antennas, and (2) interferers observed only by the n^{th} antenna, respectively. Following this system model, the total interference at antenna n, denoted by z_n, can be expressed as

$$z_n=\sum_{i_0\in\mathscr{S}_0} x_{0,i_0} d_{0,i_0}^{-\gamma/2} g_{0,n,i_0}+\sum_{i_n\in\mathscr{S}_n} x_{n,i_n} d_{n,i_n}^{-\gamma/2} g_{n,i_n} \tag{2}$$

where x_{k,i_k} indicates the emission from the i_k^{th} interferer in set $\mathscr{S}_k$, and x_{k,i_0} indicates the emission from the i_0^{th} interferer in set $\mathscr{S}_0$. The emission from each interferer is assumed to be identically and independently distributed. g_{k,i_k} is the Rayleigh fading channel between the i_k^{th} interferer and the k^{th} receive antenna, the other receive antennas do not observe interferer i_k. Since the interferers in set $\mathscr{S}_0$ are observed by all receive antennas, the Rayleigh

fading channel between the interferer and the k^{th} receive antenna is denoted by g_{0,k,i_0}. d_{n,i_n} denotes the distance between the i_n interferer in set $\mathscr{S}_n$ and the receiver. $\gamma/2$ is the amplitude path-loss parameter, which means that the power path-loss coefficient is γ.

In the next two sections, we derive the outage performance of various diversity combining techniques. The expression for the outage probability of each receiver allows us to study the impact of network parameters such as interferer density, path-loss exponent and interferer field correlation on outage performance.

IV. Outage performance of pre-detection diversity combining

In this section, we evaluate the outage performance of pre-detection diversity combining receivers, placed within a field of Poisson distributed interferers as described in Section III. In pre-detection diversity combining, the signal samples at the multiple receive antennas are combined before symbol detection. The relevant components of such a receiver are shown in Figure 2. During diversity combining, the signal output from each antenna n is multiplied by a corresponding complex scalar weight w_n and the result is summed across all N receive antennas. The key behind different diversity combining schemes lies in the selection of the weights $w_i \ \forall \ i = 1,2,\ldots,N$, henceforth denoted in vector form as the *weight vector* $\mathbf{w} = [w_1 \quad w_2 \quad \ldots \quad w_n]^T$.

For a general weight vector $\mathbf{w}$, the output at the diversity combiner can be expressed as

$$v = \mathbf{w}^T\mathbf{y} \tag{3}$$

$$= s\sum_{n=1}^{N} w_n h_n + \sum_{n=1}^{N} w_n z_n \tag{4}$$

$$= s\sum_{n=1}^{N} w_n h_n + \sum_{n=1}^{N}\sum_{i_0\in\mathscr{S}_0} x_{0,i_0} d_{0,i_0}^{-\gamma/2} w_n g_{0,n,i_0} + \sum_{n=1}^{N}\sum_{i_n\in\mathscr{S}_n} x_{n,i_n} d_{n,i_n}^{-\gamma/2} w_n g_{n,i_n} \tag{5}$$

$$= s\sum_{n=1}^{N} w_n h_n + \sum_{i_0\in\mathscr{S}_0} x_{0,i_0} d_{0,i_0}^{-\gamma/2} \sum_{n=1}^{N} w_n g_{0,n,i_0} + \sum_{n=1}^{N}\sum_{i_n\in\mathscr{S}_n} x_{n,i_n} d_{n,i_n}^{-\gamma/2} w_n g_{n,i_n}. \tag{6}$$

The SIR at combiner output can then be written as

$$\mathrm{SIR}_{\mathbf{w}} = \frac{E_s \left| \sum_{n=1}^{N} w_n h_n \right|^2}{\left| \left(\sum_{i_0 \in \mathscr{S}_0} x_{0,i_0} d_{0,i_0}^{-\gamma/2} \left(\sum_{n=1}^{N} w_n g_{0,n,i_0} \right) \right) + \sum_{n=1}^{N} \sum_{i_n \in \mathscr{S}_n} x_{n,i_n} d_{n,i_n}^{-\gamma/2} w_n g_{n,i_n} \right|^2}. \tag{7}$$

where $E_s = |s|^2$. We define the outage probability as

$$P_{\mathbf{w}}^{\mathrm{out}}(\theta) = \mathbb{E}_{\mathrm{SIR}_{\mathbf{w}}} [\mathbb{P}(\mathrm{SIR}_{\mathbf{w}} < \theta)] \tag{8}$$

where θ is the SIR threshold for correct detection. The outage probability can be written as

$$P_{\mathbf{w}}^{\mathrm{out}}(\theta) = \mathbb{E} \left[\mathbb{P} \left(\frac{E_s \left| \sum_{n=1}^{N} w_n h_n \right|^2}{\left| \left(\sum_{i_0 \in \mathscr{S}_0} x_{0,i_0} d_{0,i_0}^{-\gamma/2} \left(\sum_{n=1}^{N} w_n g_{0,n,i_0} \right) \right) + \sum_{n=1}^{N} \sum_{i_n \in \mathscr{S}_n} x_{n,i_n} d_{n,i_n}^{-\gamma/2} w_n g_{n,i_n} \right|^2} < \theta \right) \right] \tag{9}$$

$$= \mathbb{E} \left[\mathbb{P} \left(\left| \sum_{i \in U \mathscr{S}_0} x_{0,i_0} \| r_{0,i_0} \|^{-\gamma/2} \sum_{n=1}^{N} w_n g_{0,n,i_0} + \sum_{n=1}^{N} \sum_{i_n \in \mathscr{S}_n} x_{n,i_n} \| r_{n,i_n} \|^{-\gamma/2} g_{n,i_n} \right| > \frac{\sqrt{E_s} \left| \sum_{n=1}^{N} w_n h_n \right|}{\sqrt{\theta}} \right) \right]. \tag{10}$$

As the union of independent Poisson point processes is another Poisson point process with intensity equal to the sum of intensities of the constituent processes [27], we write (10) as

$$P_{\mathbf{w}}^{\mathrm{out}}(\theta) = \mathbb{E} \left[\mathbb{P} \left(\left| \sum_{i \in \cup_{n=0}^{N} \mathscr{S}_n} x_i' (d_i')^{-\gamma/2} g_i' \right| > \frac{\sqrt{E_s} \left| \sum_{n=1}^{N} w_n h_n \right|}{\sqrt{\theta}} \right) \right] \tag{11}$$

where d_i' is the distance from origin of each point (indexed by i) in the combined process. x_i' is a single random variable indicating the emissions from all interferers. g_i' is a $N+1$ term complex Gaussian mixture random variable with variances $\|\mathbf{w}\|^2\sigma^2$, $|w_1|^2\sigma^2$, $|w_2|^2\sigma^2$, … $|w_N|^2\sigma^2$, and mixing probabilities $\frac{\lambda_0}{\sum_{n=0}^{N}\lambda_n}$, $\frac{\lambda_1}{\sum_{n=0}^{N}\lambda_n}$, … $\frac{\lambda_n}{\sum_{n=0}^{N}\lambda_n}$, respectively. Theorem 1.4.2 in [28] shows that a random variable of the form $\sum_{i \in \cup_{n=0}^{N} \mathscr{S}_n} x_i' \| r_i' \|^{-\gamma/2} g_i'$ follows the symmetric alpha-stable distribution with stability parameter $\alpha = \frac{4}{\gamma}$ and scale parameter $p_\sigma = C_\alpha^{-1} E[g_i'^{\alpha}]^{\frac{1}{\alpha}}$,

where C_α is a constant defined as

$$C_\alpha = \begin{cases} \frac{1-\alpha}{2\Gamma(2-\alpha)\cos(\pi\alpha/2)} & \text{if} \quad \alpha \neq 1 \\ \frac{2}{\pi} & \text{if} \quad \alpha = 1 \end{cases}. \tag{12}$$

Property 1.2.15 in [28] states that the complementary cumulative distribution function (ccdf) for an alpha-stable distributed random variable R with stability parameter $0 < \alpha < 2$ and scale parameter $p_\sigma > 0$ and a threshold $T >> 0$, the following approximation holds well

$$\lim_{T\to\infty} \mathbb{P}\{R > T\} = C_\alpha {p_\sigma}^\alpha T^{-\alpha}. \tag{13}$$

Using Theorem 1.4.2 from [28], (12), and (13), we express (11) as

$$P_{\mathbf{w}}^{\text{out}}(\theta) \approx \pi \left(\sum_{n=0}^{N} \lambda_n \right) \mathbb{E}\left[(x_0')^\alpha \right] \mathbb{E}\left[(g_0')^\alpha \right] \mathbb{E}\left[\left(\frac{\sqrt{E_s} \left| \sum_{n=1}^{N} w_n h_n \right|}{\sqrt{\theta}} \right)^{-\alpha} \right] \tag{14}$$

where $\alpha = \frac{4}{\gamma}$, and $\Gamma(\cdot)$ is the well-known Gamma function [29]. Note that 14 is applicable only when $\alpha > 1$, consequently, our analysis is applicable only for pathloss $\gamma > 4$. The ccdf result used in (14) is also an approximate result and matches the true ccdf closely when θ is small, consequently, our results are useful in low-outage regimes. In section III, we assume that the fast-fading channel between transmitter and receiver, and interferer and receiver is a complex Gaussian random variable; i.e., the random variables g_0' and $h_n \ \forall \ n = 1, \cdots, N$ follow the Gaussian distribution. Taking expectation with respect to g_0' and $h_n \ \forall \ n = 1, \cdots, N$ in (14), we get

$$P_{\mathbf{w}}^{\text{out}}(\theta) \approx \pi 2^{\frac{\alpha}{2}} \Gamma\left(\frac{1+\alpha}{2}\right) \mathbb{E}[X^\alpha] \left(\left(\sum_{n=1}^{N} \lambda_n |w_n|^\alpha \sigma_I^\alpha \right) + \lambda_0 \|\mathbf{w}\|_2^\alpha \sigma_I^\alpha \right) \mathbb{E}\left[\left(\frac{\sqrt{E_s} \left| \sum_{n=1}^{N} w_n h_n \right|}{\sqrt{\theta}} \right)^{-\alpha} \right] \tag{15}$$

$$= \pi \Gamma(1-\alpha/2) E_s^{-\frac{\alpha}{2}} \sigma_S^{-\alpha} \sigma_I^\alpha \Gamma\left(\frac{1+\alpha}{2}\right) \mathbb{E}[X^\alpha] \frac{\sum_{n=1}^{N} \lambda_n |w_n|^\alpha + \lambda_0 \|\mathbf{w}\|_2^\alpha}{\|\mathbf{w}\|_2^\alpha} \theta^{\frac{\alpha}{2}}. \tag{16}$$

From (16) we can make intuitively satisfying observations such as the outage probability is directly proportional to the detection SIR threshold θ, and interferer density λ_n $(n = 0, 1, \ldots, N)$,

whereas it is inversely proportional to the signal power E_s. The following subsections analyze the outage probability for some typical diversity combining receivers.

A. Fixed Weight Combining

The outage probability for a receiver using a weight vector $\mathbf{w}$ is provided in (16). In fixed weight diversity combining, $\mathbf{w}$ remains constant and independent from the received signal. In a special case of fixed weight combining, known as equal gain combining, every element of the weight vector is equal. The outage performance of such a scheme is given as

$$P_{EGC}^{\text{out}}(\theta) \approx \pi E_s^{-\frac{\alpha}{2}} \sigma_S^{-\alpha} \sigma_I^{\alpha} \Gamma(\frac{1+\alpha}{2}) \Gamma(1-\alpha/2) \mathbb{E}[X^{\alpha}] \frac{\sum_{n=1}^{N} \lambda_n + \lambda_0 N^{\frac{\alpha}{2}}}{N^{\frac{\alpha}{2}}} \theta^{\frac{\alpha}{2}}. \tag{17}$$

We consider a reasonable scenario where the intensity of each of the interferer sets $\mathscr{S}_n$ $\forall$ $n = 1, \ldots, N$ is equal to λ_e. Applying to (17), we get

$$P_{\text{EGC}}^{\text{out}}(\theta) \approx \pi E_s^{-\frac{\alpha}{2}} \sigma_S^{-\alpha} \sigma_I^{\alpha} \Gamma(1+\alpha/2) \Gamma(1-\alpha/2) \mathbb{E}[X^{\alpha}] (\lambda_e N^{1-\frac{\alpha}{2}} + \lambda_0) \theta^{\frac{\alpha}{2}}. \tag{18}$$

From (18) we can deduce that the common set of interferers does not provide any diversity gain in outage performance, while the independent set of interferers actually worsens outage performance upon increasing the number of receive antennas. This reduction in outage performance is due to *interference diversity* where increasing the number of receive antennas increases the chances that one of them might be suffering from an impulsive interference event which corrupts the entire combiner output. Also note that when interference statistics are close to Gaussian distribution the $N^{1-\frac{\alpha}{2}}$ term disappears and the equal gain combiner has no diversity gain or loss, a well-known fact [30] that helps validate our results.

Assuming that the receiver has knowledge of interference statistics, we can choose $\mathbf{w}$ to minimize the outage probability as

$$P_{\text{FWC}}^{\text{out}}(\theta) = \pi E_s^{-\frac{\alpha}{2}} \sigma_S^{-\alpha} \sigma_I^{\alpha} \Gamma(\frac{1+\alpha}{2}) \Gamma(1-\alpha/2) \mathbb{E}[X^{\alpha}] \theta^{\frac{\alpha}{2}} \min_{\mathbf{w} \in \mathbb{R}^N} \left\{ \frac{\sum_{n=1}^{N} \lambda_n |w_n|^{\alpha} + \lambda_0 \|\mathbf{w}\|_2^{\alpha}}{\|\mathbf{w}\|_2^{\alpha}} \right\}. \tag{19}$$

(19) attains its minimum value when the receiver selects the antenna with the minimum average interference power. Since interference power is directly proportional to the intensity,

we can write (19) as

$$P_{\text{FWC}}^{\text{out}}(\theta) = \pi E_s^{-\frac{\alpha}{2}} \sigma_S^{-\alpha} \sigma_I^{\alpha} \Gamma(\frac{1+\alpha}{2}) \Gamma(1-\alpha/2) \mathbb{E}[X^{\alpha}] \, \theta^{\frac{\alpha}{2}} \min_{n=1,\ldots,N} \{\lambda_n + \lambda_0\}. \tag{20}$$

B. Maximum Ratio Combining

In this diversity combining technique, the receiver chooses a weight vector directly proportional to the channel conjugate and inversely proportional to the interference power [30]. Assuming *i.i.d.* interferer emissions and *i.i.d.* fading between interferer and receiver, the interference power at each antenna would be proportional to $\lambda_0 + \lambda_n$. Thus the n^{th} element of the combining weight vector w_n would be given by $w_n = \frac{h_n^*}{\lambda_0 + \lambda_n}$. Again assuming that $\lambda_n = \lambda_e \ \forall \ n$, and inserting the MRC weight vector into (15), the outage probability of MRC combining can be expressed as

$$P_{\text{MRC}}^{\text{out}}(\theta) \approx \pi E_s^{-\frac{\alpha}{2}} \sigma_I^{\alpha} 2^{\frac{\alpha}{2}} \Gamma(1/2+\alpha/2) \mathbb{E}[X^{\alpha}] \, \mathbb{E}\left[\frac{\sum_{n=1}^{N} \lambda_n |h_n|^{\alpha} + \lambda_0 \|\mathbf{h}\|_2^{\alpha}}{\|\mathbf{h}\|_2^{2\alpha}} \right] \theta^{\frac{\alpha}{2}} \tag{21}$$

$$= \pi E_s^{-\frac{\alpha}{2}} \sigma_I^{\alpha} 2^{\frac{\alpha}{2}} \Gamma(1/2+\alpha/2) \mathbb{E}[X^{\alpha}] \, \mathbb{E}\left[\frac{\sum_{n=1}^{N} \lambda_n |h_n|^{\alpha}}{\|\mathbf{h}\|_2^{2\alpha}} + \frac{\lambda_0}{\|\mathbf{h}\|_2^{\alpha}} \right] \theta^{\frac{\alpha}{2}}. \tag{22}$$

For the special case where intensities of the independent set of interferers λ_n ($n = 1,2,\ldots,N$) are *all* equal to λ_e, we can simplify (21) to

$$P_{\text{MRC}}^{\text{out}}(\theta) \approx \pi E_s^{-\frac{\alpha}{2}} \sigma_I^{\alpha} 2^{\frac{\alpha}{2}} \Gamma(1/2+\alpha/2) \mathbb{E}[X^{\alpha}] \, \mathbb{E}\left[\frac{\lambda_e \|\mathbf{h}\|_{\alpha}^{\alpha}}{\|\mathbf{h}\|_2^{2\alpha}} + \frac{\lambda_0}{\|\mathbf{h}\|_2^{\alpha}} \right] \theta^{\frac{\alpha}{2}} \tag{23}$$

Note that channel diversity does provide some improvement in outage performance, especially in the case of isotropic interference.

C. Selection Combining

Selection combining is a receive diversity technique where the receiver chooses to decode the signal from one antenna [30]. The advantages of selection combining are that no gain and phase multiplication block is needed in the receiver hardware, at the cost of negatively impacting the communication performance since the signal energy from other antennas is not used. In the pre-detection diversity combining setting, we study the sub-optimal

selection combiner which selects the receive antenna with the strongest channel. In this combiner, the weight vector has value 1.0 at the antenna with the strongest channel and value 0 for the rest. Consequently, we can write the output of the diversity combiner as

$$\upsilon = \mathbf{w}^T \mathbf{y} \tag{24}$$

$$= s\frac{|h_n|^2}{\lambda_0+\lambda_n} + \frac{h_n z_n}{\lambda_0+\lambda_n} \tag{25}$$

$$= s\,h_m + z_m \tag{26}$$

where index m indicates the index of the receiver with the strongest channel; i.e., $|h_m|^2 \geq |h_n|^2$ $\forall n = 1,2,\ldots,N$. The outage probability can then be written as

$$P_{\text{SC}}^{\text{out}}(\theta) \approx \pi E_s^{-\frac{\alpha}{2}} \sigma_I^{\alpha} \Gamma(1/2+\alpha/2)\mathbb{E}\left[X^{\alpha}\right] \left(\sum_{n=0}^{N} \frac{\lambda_n+\lambda_0}{N}\right) \mathbb{E}\left[|h_m|^{-\alpha}\right] \theta^{\frac{\alpha}{2}} \tag{27}$$

$$= \pi\Gamma(1-\alpha/2)\left(\frac{\sigma_I}{\sqrt{E_s}\sigma_S}\right)^{\alpha} \Gamma(1/2+\alpha/2)\mathbb{E}\left[X^{\alpha}\right] \left(\sum_{n=0}^{N} \frac{\lambda_n+\lambda_0}{N}\right) \left(\sum_{m=0}^{N} (-1)^{m+1} \frac{\binom{N}{m}}{m^{\alpha}}\right) \theta^{\frac{\alpha}{2}}. \tag{28}$$

V. Outage probability of post-detection combining

In Section IV, we evaluated outage performance for receivers implementing a weighted combiner, as shown in Figure 2. In this section, we evaluate the outage performance for a receiver that implements selection combining after performing detection. The block diagram for this receiver is shown in Figure 3. This receiver has a higher computational complexity since it implements a detection block for each antenna as opposed to the receiver in Figure 2 which implements only one detection block. Such a receiver attempts to detect the transmitted signal individually at each antenna and then selects the output based on the decoded signals. This may be accomplished by taking a majority vote among receivers, estimating the SIR at each decoded output, or by using a error-checking code. We assume a scenario in which the receiver can successfully decode, if at least one of the antennas signals exhibits SIR greater than the detection threshold. This receiver may not be practical to implement in some wireless systems, but the analysis provides us with a lower bound on outage performance. Under these conditions, such a receiver would be in outage only if the per-antenna SIR is below the detection threshold at every antenna. The probability of this

event can be expressed as

$$
\begin{aligned}
P_{\mathrm{PDC}}^{\mathrm{out}} &= \mathbb{P}\{\mathrm{SIR}_1 < \theta, \mathrm{SIR}_2 < \theta, \ldots, \mathrm{SIR}_n < \theta\} \\
&= \mathbb{E}\left[\mathbb{P}\left\{\frac{E_s |h_1|^2}{\left|\left(\sum_{i_0\in\mathscr{S}_0} x_{0,i_0} d_{0,i_0}^{-\gamma/2} h_{0,1,i_0}\right) + \sum_{i_1\in\mathscr{S}_1} x_{1,i_1} d_{1,i_1}^{-\gamma/2} h_{1,i_1}\right|^2} < \theta, \ldots \right.\right. \\
&\qquad \left.\left. \ldots, \frac{E_s |h_n|^2}{\left|\left(\sum_{i_0\in\mathscr{S}_0} x_{0,i_0} d_{0,i_0}^{-\gamma/2} h_{0,n,i_0}\right) + \sum_{i_n\in\mathscr{S}_n} x_{n,i_n} d_{n,i_n}^{-\gamma/2} h_{n,i_n}\right|^2} < \theta \right\}\right] \qquad (29) \\
&= \mathbb{E}\left[\mathbb{P}\left\{|h_1|^2 < \frac{\theta\left|\left(\sum_{i_0\in\mathscr{S}_0} x_{0,i_0} d_{0,i_0}^{-\gamma/2} h_{0,1,i_0}\right) + \sum_{i_1\in\mathscr{S}_1} x_{1,i_1} d_{1,i_1}^{-\gamma/2} h_{1,i_1}\right|^2}{E_s}, \ldots \right.\right. \\
&\qquad \left.\left. \ldots, |h_n|^2 < \frac{\theta\left|\left(\sum_{i_0\in\mathscr{S}_0} x_{0,i_0} d_{0,i_0}^{-\gamma/2} h_{0,n,i_0}\right) + \sum_{i_n\in\mathscr{S}_n} x_{n,i_n} d_{n,i_n}^{-\gamma/2} h_{n,i_n}\right|^2}{E_s} \right\}\right] \qquad (30) \\
&= \mathbb{E}\left[\prod_{n=1}^{N}\left(1 - e^{\frac{\theta}{E_s\sigma_H^2}\left|\sum_{i_0\in\mathscr{S}_0} x_{0,i_0} d_{0,i_0}^{-\gamma/2} h_{0,n,i_0} + \sum_{i_n\in\mathscr{S}_n} x_{n,i_n} d_{n,i_n}^{-\gamma/2} h_{n,i_n}\right|^2}\right)\right] \qquad (31) \\
&\approx \mathbb{E}\left[\prod_{n=1}^{N}\left(1 - e^{\frac{\theta}{E_s\sigma_H^2}\sum_{i_0\in\mathscr{S}_0}|x_{0,i_0}|^2 d_{0,i_0}^{-\gamma}|h_{0,n,i_0}|^2 + \sum_{i_n\in\mathscr{S}_n}|x_{n,i_n}|^2 d_{n,i_n}^{-\gamma}|h_{n,i_n}|^2}\right)\right]. \qquad (32)
\end{aligned}
$$

We proceed by setting the number of receive antennas, $N=2$, in order to facilitate brevity and comprehension of this derivation. Later, we will provide the outage probability for any number of receive antennas. Assuming $N=2$, we can expand (31) as

$$
\begin{aligned}
P_{\mathrm{PDC}}^{\mathrm{out}} = 1 &- \mathbb{E}\left[e^{\frac{\theta}{E_s\sigma_H^2}\left(\sum_{i_0\in\mathscr{S}_0}|x_{0,i_0}|^2 d_{0,i_0}^{-2\gamma}|g_{0,1,i_0}|^2 + \sum_{i_1\in\mathscr{S}_n}|x_{1,i_1}|^2 d_{1,i_1}^{-\gamma}|g_{1,i_1}|^2\right)}\right] \\
&- \mathbb{E}\left[e^{\frac{\theta}{E_s\sigma_H^2}\left(\sum_{i_0\in\mathscr{S}_0}|x_{0,i_0}|^2 d_{0,i_0}^{-\gamma}|g_{0,2,i_0}|^2 + \sum_{i_2\in\mathscr{S}_2}|x_{2,i_2}|^2 d_{2,i_2}^{-\gamma}|g_{2,i_2}|^2\right)}\right] \\
&+ \mathbb{E}\left[e^{\frac{\theta}{E_s\sigma_H^2}\left(\sum_{i_0\in\mathscr{S}_0}|x_{0,i_0}|^2 d_{0,i_0}^{-\gamma}(|g_{0,1,i_0}|^2 + |g_{0,2,i_0}|^2) + \sum_{i_1\in\mathscr{S}_n}|x_{1,i_1}|^2 d_{1,i_1}^{-\gamma}|g_{1,i_1}|^2 + \sum_{i_2\in\mathscr{S}_2}|x_{2,i_2}|^2 d_{2,i_2}^{-\gamma}|g_{2,i_2}|^2\right)}\right]. \qquad (33)
\end{aligned}
$$

Taking expectation over g, we get

$$P_{\text{PDC}}^{\text{out}} = 1 - \mathbb{E}\left[\prod_{i_0\in\mathscr{S}_0}\left(1+\frac{\sigma_I^2\theta X^2}{E_s\sigma_H^2}\left|x_{0,i_0}\right|^2 d_{0,i_0}^{-\gamma}\right)^{-1}\prod_{i_1\in\mathscr{S}_n}\left(1+\frac{\sigma_I^2\theta X^2}{E_s\sigma_H^2}\left|x_{1,i_1}\right|^2 d_{1,i_1}^{-\gamma}\right)^{-1}\right]$$
$$-\mathbb{E}\left[\prod_{i_0\in\mathscr{S}_0}\left(1+\frac{\sigma_I^2\theta X^2}{E_s\sigma_H^2}\left|x_{0,i_0}\right|^2 d_{0,i_0}^{-\gamma}\right)^{-1}\prod_{i_2\in\mathscr{S}_2}\left(1+\frac{\sigma_I^2\theta X^2}{E_s\sigma_H^2}\left|x_{2,i_2}\right|^2 d_{2,i_2}^{-\gamma}\right)^{-1}\right]$$
$$+\mathbb{E}\left[\prod_{i_0\in\mathscr{S}_0}\left(1+\frac{\sigma_I^2\theta X^2}{E_s\sigma_H^2}\left|x_{0,i_0}\right|^2 d_{0,i_0}^{-\gamma}\right)^{-2}\prod_{i_1\in\mathscr{S}_n}\left(1+\frac{\sigma_I^2\theta X^2}{E_s\sigma_H^2}\left|x_{1,i_1}\right|^2 d_{1,i_1}^{-\gamma}\right)^{-1}\times\right.$$
$$\left.\prod_{i_2\in\mathscr{S}_2}\left(1+\frac{\sigma_I^2\theta X^2}{E_s\sigma_H^2}\left|x_{2,i_2}\right|^2 d_{2,i_2}^{-\gamma}\right)^{-1}\right]. \tag{34}$$

Using the point generating functional property of Poisson point processes [31], we can write the outage probability $P_{\text{PDC}}^{\text{out}}$ as

$$P_{\text{PDC}}^{\text{out}} = \mathbb{E}\left[1 - e^{(\lambda_0+\lambda_1)\int_{\mathbf{t}\in\mathscr{R}} 1-\left(1+\frac{\sigma_I^2\theta X^2}{E_s\sigma_H^2}\|t\|^{-\gamma}\right)^{-1} d\mathbf{t}} - e^{(\lambda_0+\lambda_2)\int_{\mathbf{t}\in\mathscr{R}} 1-\left(1+\frac{\sigma_I^2\theta X^2}{E_s\sigma_H^2}\|t\|^{-\gamma}\right)^{-1} d\mathbf{t}}\right.$$
$$\left.+e^{\lambda_1\int_{\mathbf{t}\in\mathscr{R}} 1-\left(1+\frac{\sigma_I^2\theta X^2}{E_s\sigma_H^2}\|t\|^{-\gamma}\right)^{-1} d\mathbf{t}} e^{\lambda_2\int_{\mathbf{t}\in\mathscr{R}} 1-\left(1+\frac{\sigma_I^2\theta X^2}{E_s\sigma_H^2}\|t\|^{-\gamma}\right)^{-1} d\mathbf{t}} e^{\lambda_0\int_{\mathbf{t}\in\mathscr{R}} 1-\left(1+\frac{\sigma_I^2\theta X^2}{E_s\sigma_H^2}\|t\|^{-\gamma}\right)^{-2} d\mathbf{t}}\right]. \tag{35}$$

After integration, subsequent simplification, and noting that in a low outage regime, the operand in the exponential is close to 0, we approximate the outage probability as

$$P_{\text{PDC}}^{\text{out}} \approx \frac{(1+\alpha/2)\alpha\pi^2}{\sin(\alpha\pi)}\left(\frac{\sigma_I\mathbb{E}[X]}{E_s\sigma_H}\right)^{\alpha}\lambda_0\theta^{\alpha/2} + \left(\frac{\alpha\pi^2}{4\sin(\alpha\pi)}\right)^2\lambda_1\lambda_2\left(\frac{\sigma_I\mathbb{E}[X]}{E_s\sigma_H}\right)^{2\alpha}\theta^{\alpha} \tag{36}$$

(36) shows the contribution to the outage probability from the interferer set $\mathscr{S}_0$ and the interferer sets $\mathscr{S}_n$ for $n=1,\ldots,N$. Extending this result to an N antenna receiver leads to a more involved outage probability expression comprising of a summation of terms containing $\theta^{k\alpha/2}$ with $k=1,\ldots,N$. The $\theta^{\alpha/2}$ term is the outage component purely due to interferers from $\mathscr{S}_0$, the $\theta^{N\alpha/2}$ term is purely due to interferers from $\mathscr{S}_n$ for $n=1,\ldots,N$, and the $\theta^{k\alpha 2}$ terms are due to interference from all the sets $\mathscr{S}_n$ for $n=0,\ldots,N$. We approximate the outage probability by keeping only the $\theta^{\alpha/2}$ and $\theta^{N\alpha/2}$ terms and ignoring the rest. The justification is that when $\lambda_0\neq 0$, the $\theta^{\alpha/2}$ term (outage from isotropic interference) dominates the overall sum, and when $\lambda_0=0$, the outage probability reduces to contain only the $\theta^{N\alpha/2}$ term (outage

TABLE II
PARAMETER VALUES USED IN SIMULATIONS.

Parameter	Description	Value
λ_{tot}	Per-antenna total intensity of interferers	0.001
γ	Power path-loss exponent	6
$\mathbb{E}[X]$	Mean amplitude of interferer emissions	1.0
σ_H	Variance of in-phase and quadrature components of the fading channel	1.0
τ	Threshold parameter for hard-limiting combiner	1.0
η	Decay parameter for soft-limiting combiner	2.0

from independent interference). Thus, by continuing the derivation from (31) for $N>2$ and keeping only the two significant terms, we get the outage probability as

$$P_{\text{PDC}}^{\text{out}} \approx \left(\sum_{m=1}^{N}\binom{N}{m}\frac{(-1)^{m+1}(m-1+\alpha/2)!\pi^2}{4(m-1)!\sin(\alpha\pi)}\right)\lambda_0\left(\frac{\sigma_I\mathbb{E}[X]}{E_s\sigma_H}\right)^{\alpha}\theta^{\alpha/2} + \left(\frac{\alpha\pi^2}{4\sin(\alpha\pi)}\right)^{N}\left(\prod_{n=1}^{N}\lambda_n\right)\left(\frac{\sigma_I\mathbb{E}[X]}{E_s\sigma_H}\right)^{N\alpha}\theta^{N\alpha/2}. \quad (37)$$

It is important to note that we get a full diversity order if there are no common interferers. Full diversity order denotes that the outage probability decreases exponentially as the number of receive antenna increases. However, when interference is spherically isotropic, increasing the number of receiver antennas does not lead to an exponential decrease in outage probability of PDC .

VI. OUTAGE PERFORMANCE COMPARISON OF DIVERSITY COMBINING SCHEMES

To validate our outage probability derivations, we numerically simulate a multi-antenna receiver located within a field of Poisson distributed interferers. We transmit a $16-$QAM signal and interference is simulated according to the system model described in Section III. The SINR threshold is set to 3dB. Based on the average signal energy and modulation index, any desired SIR threshold for correct detection can be calculated and plugged into the derived outage probability expressions to compare with simulated results. Table II lists the various parameter values used in simulations.

Figure 4 shows the impact of spatial dependence on outage probability of the various

diversity combining receivers. In Figure 4, the interferer sets observable by a single antenna have intensities $\lambda_i (i = 1, \ldots, N)$ set to the same value, denoted by λ_e. $\lambda_0 + \lambda_e$ is also set to a fixed value 0.001, so that the total interference observed by each antenna has the same power. Varying λ_0 from 0.0 to 0.001 essentially changes the interference statistics from spatially independent to spherically isotropic. Increasing spatial dependence in interference negatively impacts the communication performance of all receiver algorithms. In interference with low spatial dependence, PDC receiver has the best performance, while the other pre-detection receivers still exhibit poor performance. This shows that exploiting channel diversity in conventional multi-antenna receivers may not compensate for impulsive interference.

Figures 5, 6, and 7 show the impact of receive antennas on outage probability. In Figure 5, we simulate spatially independent interference by setting $\lambda_0 = 0$ and $\lambda_e = 0.001$. In Figure 6, we set $\lambda_e = 0$ and $\lambda_0 = 0.001$ to simulate spherically isotropic interference. It is interesting to see that the diversity gain is lost in all algorithms in the presence of spherically isotropic interference. In Figure 7 we simulate partial spatial dependence by setting $\lambda_0 = 5 \times 10^{-5}$ and $\lambda_e = 9.5 \times 10^{-4}$. Even a low amount of spatial dependence in interference can severely reduce the diversity gain of these receivers. In all of these figures, we see that the theoretical expressions derived in Sections IV and V match very well to the simulated receiver. The theoretical expressions are useful as they allow us to analyze the impact of parameters such as γ, on the diversity performance of typical multi-antenna receivers.

VII. Novel diversity combining algorithms to mitigate impulsive interference

In Section V, we observe that the post-detection combining receiver outperforms pre-detection diversity combining algorithms in the presence of impulsive interference, especially when interference exhibits low spatial dependence across receive antennas. However, this improvement comes at the cost of deploying multiple signal decoding blocks in the receiver hardware as shown in Figure 3. In this section, we propose alternative pre-detection diversity combining algorithms designed with the knowledge that interference is impulsive in nature.

A. Hard-limiting combiner

Pre-detection combiners do not distinguish between an antenna suffering from an impulsive interference event, and an antenna not observing impulsive interference. Our proposed hard-limiting receiver attempts to detect if an antenna is observing an impulsive event, and if so, removes that antenna from the combining block. Its weight vector can be written as

$$w_n^{HL} = \begin{cases} h_n^* & \text{if} \quad \|y_n - \text{median}(\mathbf{y})\| \leq \tau \\ 0 & \text{if} \quad \|y_n - \text{median}(\mathbf{y})\| \geq \tau \end{cases}. \tag{38}$$

The receiver assumes that an impulsive interference event has occurred if the antenna signal significantly deviates from the median of the all the receive antenna samples. In impulsive random variables, the median is often used as a metric to denote the typical value of a signal [32]. Only antennas deemed to exhibit non-impulsive interference are used to combine the received signals using the MRC algorithm

B. Soft-limiting combiner

The hard-limiting combiner completely removes an antenna from the diversity combination process if it detects the presence of an interference impulse event. The soft-limiting combiner, on the other hand, gradually reduces the weighting of an antenna if it estimates an impulse event at the antenna. The soft-limiting weight vector is given as

$$w_n^{SL} = e^{-\eta\|y_n - \text{median}(\mathbf{y})\|} h_n^*. \tag{39}$$

Here the MRC algorithm is modified to reduce the weight of an antenna if its received signal deviates highly from the signals at other antennas. Unlike hard-limiting combining, the weight is gradually reduced as deviation increases. Both these proposed algorithms are modifications to the MRC receiver. These combiners are non-linear in nature and their outage probability expressions are mathematically intractable. We choose values of τ and η that show improved performance compared to pre-detection diversity combining schemes. Subsequently, evaluating the optimal value of parameters τ and η, or adaptively tuning these parameters depending on noise statistics are interesting avenues of future work.

Using the parameters from Table II, we show the outage performance of our proposed algorithms in Figure 8 and 9. At low spatial dependence in interference, our proposed algorithms outperform conventional pre-detection diversity combining receivers, while providing a trade-off between communication performance and computational complexity. Figure 10 shows that the outage performance of these algorithms in Gaussian distributed interference matches the performance of MRC receiver. The variance of Gaussian distributed interference is chosen as 0.05, so that the outage probabilities are in the same range as other figures.

VIII. Conclusion

In this paper, we derive outage probability expressions for various diversity receivers in the presence of interference, such as equal gain combining, fixed weight combining, maximum ratio combining, selection combining, and post-detection combining. We use a generalized framework to model spatially dependent wireless interference with joint statistics in a continuum from spatially independent to spherically isotropic. While this framework can model interference in common scenarios which usually fall at either extreme of this continuum, it proves advantageous when modeling scenarios which fall within the continuum.

The post-detection diversity combiner exhibits significantly better outage performance compared to the pre-detection diversity combining receivers. In spatially independent interference, the post-detection combiner achieves full diversity order in outage performance. This diversity order is quickly lost upon increasing spatial dependence in interference observed across receive antennas. The post-detection combiner suffers from high computational complexity requirements as it requires a symbol decoding block for each receive antenna, compared to the pre-detection combiner which requires one symbol decoding block regardless of the number of receive antennas. We propose two novel diversity combining algorithms which improve upon the outage performance of pre-detection diversity combining receivers, while using the same amount of computational complexity. Our results can inform analysis of communication performance vs. computational complexity tradeoffs of multi-antennas receivers designed to operate in the presence of impulsive interference.

REFERENCES

[1] M. Haenggi and R. K. Ganti, "Interference in large wireless networks," in *Foundations and Trends in Networking*. Now Publishers Inc., 2008, vol. 3, no. 2, pp. 127–248.

[2] D. Cox, "Cochannel interference considerations in frequency reuse small-coverage-area radio systems," *IEEE Transactions on Communications*, vol. 30, pp. 135– 142, Jan 1982.

[3] J. Shi, A. Bettner, G. Chinn, K. Slattery, and X. Dong, "A study of platform EMI from LCD panels - impact on wireless, root causes and mitigation methods," in *Proc. IEEE International Symposium on Electromagnetic Compatibility*, vol. 3, Aug. 2006, pp. 626–631.

[4] J. G. Andrews. (2011, Feb.) A tractable framework for coverage and outage in heterogeneous cellular networks. [Online]. Available: {http://users.ece.utexas.edu/~jandrews/pubs/DhillonGantiAndrews_ITA2011_Slides.pdf}

[5] J. Ilow and D. Hatzinakos, "Analytic alpha-stable noise modeling in a Poisson field of interferers or scatterers," *IEEE Transactions on Signal Processing*, vol. 46, no. 6, pp. 1601–1611, Jun. 1998.

[6] P. A. Delaney, "Signal detection in multivariate Class-A interference," *IEEE Transactions on Communications*, vol. 43, no. 4, Feb. 1995.

[7] L. Izzo and M. Tanda, "Diversity reception of fading signals in spherically invariant noise," *IEE Proceedings-Communications*, vol. 145, no. 4, pp. 272–276, 1998.

[8] A. Rajan and C. Tepedelenlioglu, "Diversity combining over rayleigh fading channels with symmetric alpha-stable noise," *IEEE Transactions on Wireless Communications*, vol. 9, no. 9, pp. 2968–2976, 2010.

[9] C. Tepedelenlioglu and P. Gao, "On diversity reception over fading channels with impulsive noise," *IEEE Transactions on Vehicular Technology*, vol. 54, no. 6, pp. 2037–2047, Nov. 2005.

[10] J. Haring and A. J. H. Vinck, "Performance bounds for optimum and suboptimum reception under class-A impulsive noise," *IEEE Transactions for Communications*, vol. 50, no. 7, pp. 1130– 1136, Jul. 2002.

[11] A. Chopra, K. Gulati, B. L. Evans, K. R. Tinsley, and C. Sreerama, "Performance bounds of MIMO receivers in the presence of radio frequency interference," in *Proc. IEEE International Conference on Acoustics, Speech and Signal Processing*, Apr. 2009, pp. 2817–2820.

[12] K. F. McDonald and R. S. Blum, "A statistical and physical mechanisms-based interference and noise model for array observations," *IEEE Transactions on Signal Processing*, vol. 48, pp. 2044–2056, July 2000.

[13] A. Kyung Seung and R. W. Heath, "Performance analysis of maximum ratio combining with imperfect channel estimation in the presence of cochannel interferences," *IEEE Transactions on Wireless Communications*, vol. 8, no. 3, pp. 1080–1085, Mar. 2009.

[14] O. B. S. Ali, C. Cardinal, and F. Gagnon, "Performance of optimum combining in a poisson field of interferers and rayleigh fading channels," *IEEE Transactions on Wireless Communications*, vol. 9, no. 8, pp. 2461–2467, 2010.

[15] M. J. Dumbrill and I. J. Rees, "Sectorized cellular radio base station antenna," U.S. Patent 5 742 911, 1998.

[16] T.-S. Lee and Z. S. Lee, "A sectorized beamspace adaptive diversity combiner for multipath environments," *IEEE Transactions on Vehicular Technology*, vol. 48, no. 5, pp. 1503–1510, 1999.

[17] X. Yang and A. Petropulu, "Co-channel interference modeling and analysis in a Poisson field of interferers in wireless communications," *IEEE Transactions on Signal Processing*, vol. 51, Jan. 2003.

[18] K. F. McDonald and R. S. Blum, "A statistical and physical mechanisms-based interference and noise model for array observations," *IEEE Transactions on Signal Processing*, vol. 48, pp. 2044 – 2056, Jul. 2000.

[19] J. G. Andrews, "Interference cancellation for cellular systems: A contemporary overview," *IEEE Wireless Communications Magazine*, vol. 12, no. 2, pp. 19–29, Apr. 2005.

[20] K. Gulati, B. Evans, J. Andrews, and K. Tinsley, "Statistics of co-channel interference in a field of Poisson and Poisson-Poisson clustered interferers," *IEEE Transactions on Signal Processing*, vol. 58, Dec. 2010.

[21] A. Hasan and J. G. Andrews, "The guard zone in wireless ad hoc networks," *IEEE Transactions on Wireless Communications*, Mar. 2007.

[22] F. Baccelli and B. Błaszczyszyn, "Stochastic geometry and wireless networks, volume 2 — applications," in *Foundations and Trends in Networking*. Now Publishers Inc., 2009, vol. 4, no. 1–2, pp. 1–312.

[23] D. Middleton, "Non-Gaussian noise models in signal processing for telecommunications: New methods and results for class A and class B noise models," *IEEE Transactions on Information Theory*, vol. 45, no. 4, May 1999.

[24] A. Rabbachin, T. Quek, S. Hyundong, and M. Win, "Cognitive network interference," *IEEE Journal on Selected Areas in Communications*, vol. 29, no. 2, Feb. 2011.

[25] A. Goldsmith, *Wireless Communications*. Cambridge University Press, 2005.

[26] F. Baccelli and B. Błaszczyszyn, "Stochastic geometry and wireless networks, volume 1 — theory," in *Foundations and Trends in Networking*. Now Publishers Inc., 2009, vol. 3, no. 3–4, pp. 249–449.

[27] F. Baccelli, M. Klein, M. Lebourges, and S. Zuyev, "Stochastic geometry and architecture of communication networks," *Journal of Telecommunication Systems*, vol. 7, pp. 209–227, Jun. 1997.

[28] G. Samorodnitsky and M. S. Taqqu, *Stable Non-Gaussian Random Processes: Stochastic Models with Infinite Variance*. Chapman and Hall, New York, 1994.

[29] M. Abramowitz and I. A. Stegun, *Handbook of mathematical functions with formulas, graphs, and mathematical tables*. Courier Dover Publications, 1964, vol. 55.

[30] E. Biglieri, R. Calderbank, A. Constantinides, A. Goldsmith, A. Paulraj, and H. V. Poor, *MIMO Wireless Communications*, 2007.

[31] R. Ganti and M. Haenggi, "Interference and outage in clustered wireless ad hoc networks," *IEEE Transactions on Information Theory*, vol. 55, no. 9, pp. 4067–4086, Sep. 2009.

[32] M. Nassar, K. Gulati, A. K. Sujeeth, N. Aghasadeghi, B. L. Evans, and K. R. Tinsley, "Mitigating near-field interference in laptop embedded wireless transceivers," in *Proc. IEEE International Conference on Acoustics, Speech and Signal Processing*, May 2008, pp. 1405–1408.

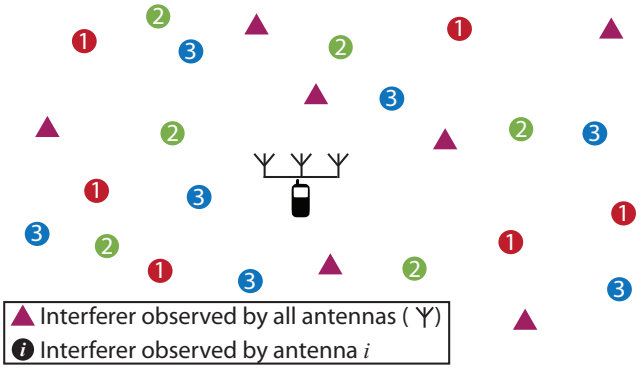

Fig. 1. System model of a 3−antenna receiver located in a field of randomly distributed interferers. The interferers are classified according to the receive antenna impacted by their emissions.

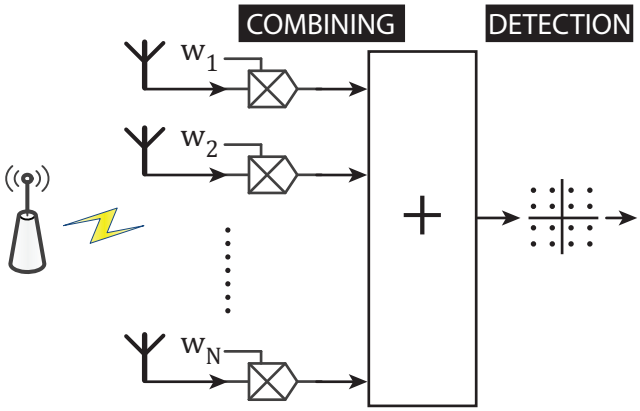

Fig. 2. Block diagram of a receiver in which diversity combining is performed before symbol detection.

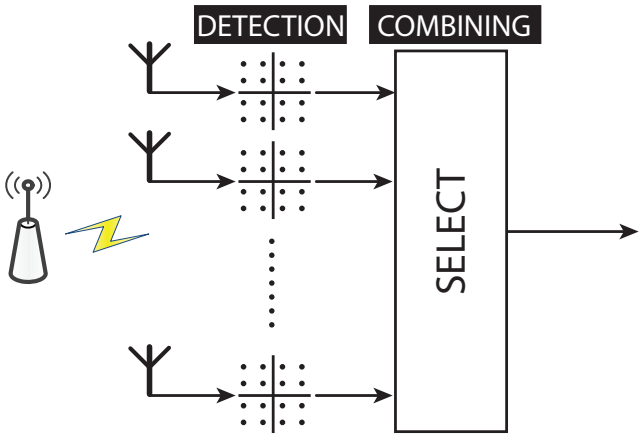

Fig. 3. Block diagram of a receiver in which diversity combining is performed after symbol detection.

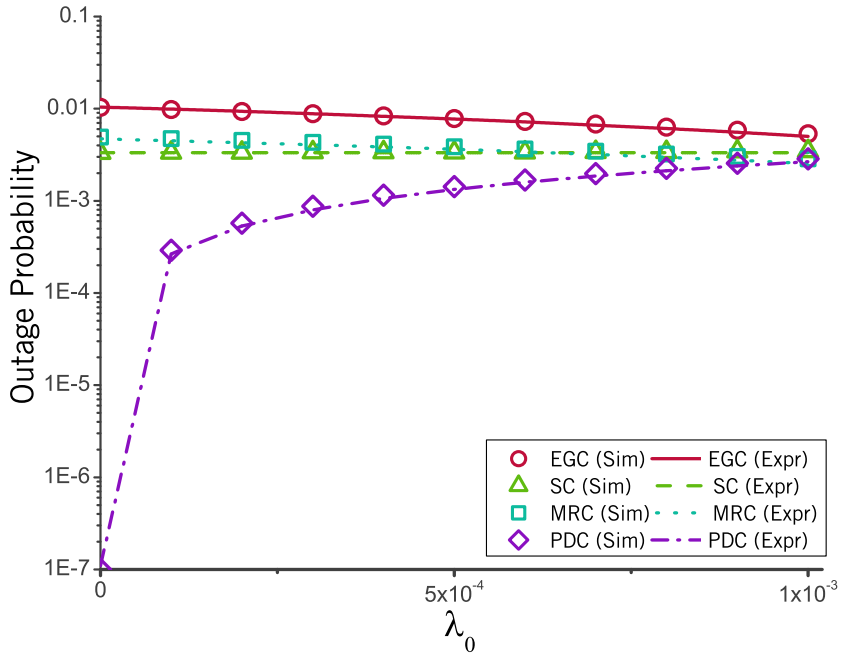

Fig. 4. Outage probability vs. λ_0 for equal gain combining (EGC), maximal ratio combining (MRC), selection combining (SC), and post-detection combining (PDC) in a 3−antenna receiver. The symbols indicate the theoretical outage probability ('Expr'), whereas the lines indicate the simulated outage probability ('Sim'). $\lambda_e = 10^{-3} - \lambda_0$.

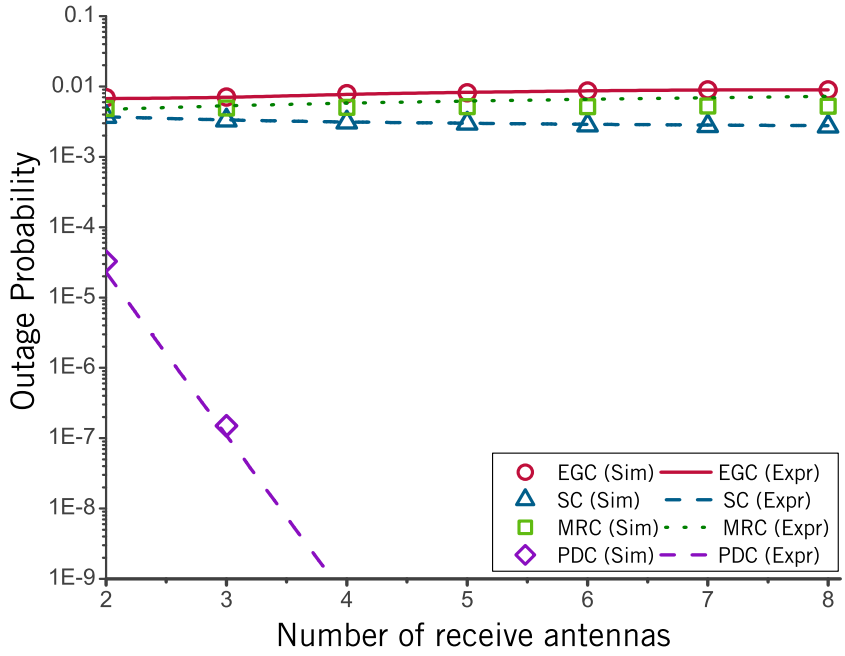

Fig. 5. Outage probability vs. number of receive antennas for for equal gain combining (EGC), maximal ratio combining (MRC), selection combining (SC), and post-detection combining (PDC) in presence of spatially independent interference. The symbols indicate the theoretical outage probability ('Expr'), whereas the lines indicate the simulated outage probability ('Sim'). Parameter values $\lambda_0 = 0, \lambda_e = 10^{-3}$ are used in simulations.

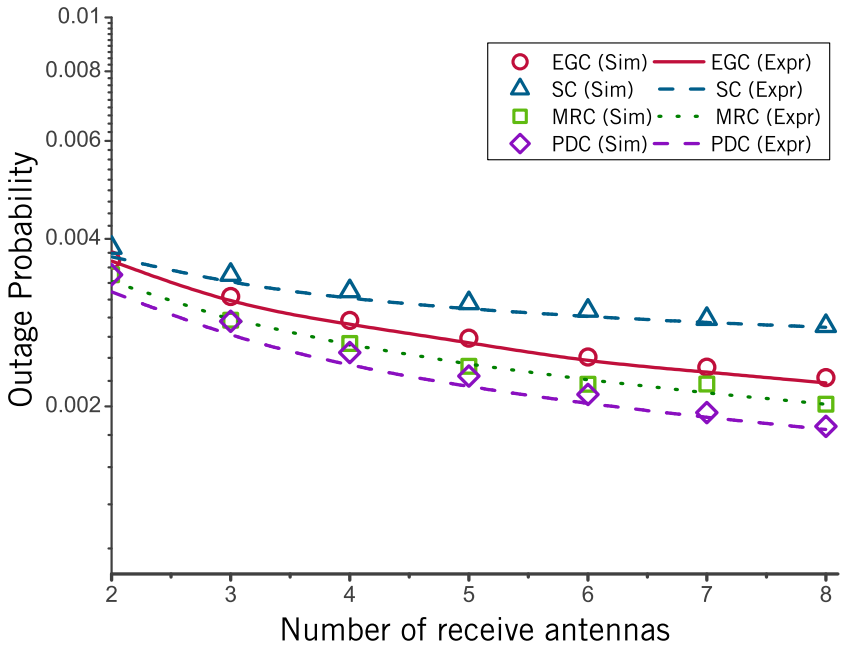

Fig. 6. Outage probability vs. number of receive antennas for for equal gain combining (EGC), maximal ratio combining (MRC), selection combining (SC), and post-detection combining (PDC) in presence of spherically isotropic interference. The symbols indicate the theoretical outage probability ('Expr'), whereas the lines indicate the simulated outage probability ('Sim'). Parameter values $\lambda_0 = 10^{-3}, \lambda_e = 0$ are used in simulations.

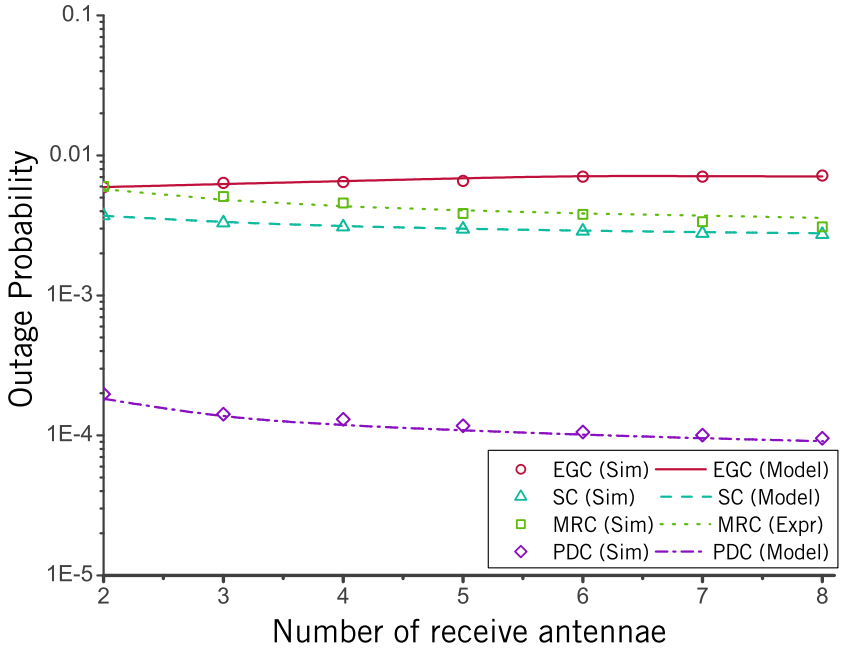

Fig. 7. Outage probability vs. number of receive antennas for equal gain combining (EGC), maximal ratio combining (MRC), selection combining (SC), and post-detection combining (PDC) in presence of partially spatially dependent interference. The symbols indicate the theoretical outage probability ('Expr'), whereas the lines indicate the simulated outage probability ('Sim'). $\lambda_0 = 5 \times 10^{-5}, \lambda_e = 9.5 \times 10^{-4}$ are used in simulations.

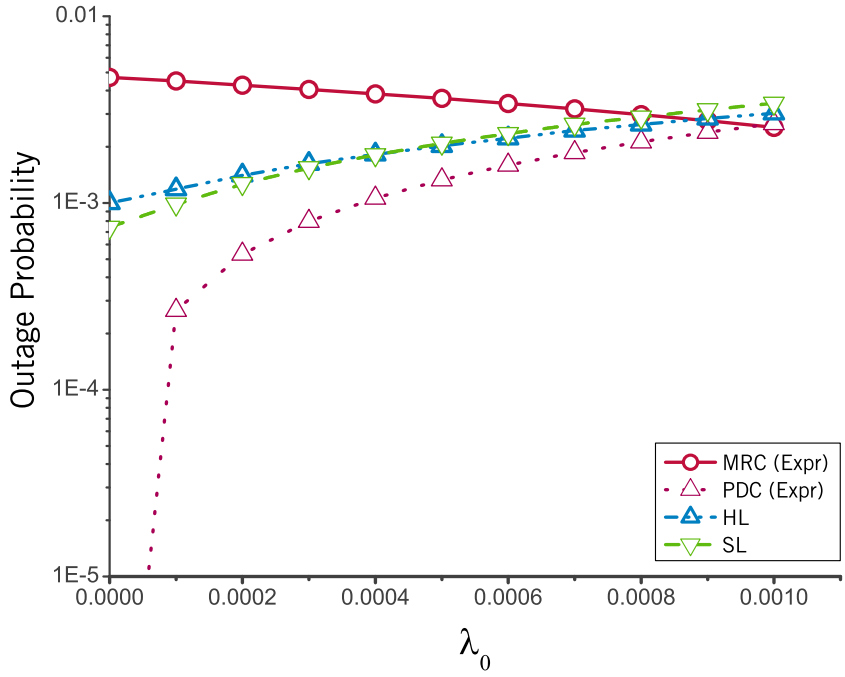

Fig. 8. Outage probability vs. λ_0 for maximal ratio combining (MRC), post-detection combining (PDC), and the novel hard-limiting (HL) and soft-limiting (SL) combiners in a 3−antenna receiver. $\lambda_e = 10^{-3} - \lambda_0$, $\tau = 1.0$, and $\eta = 2.0$. Outage probability of MRC and PDC combining is evaluated using theoretical expressions.

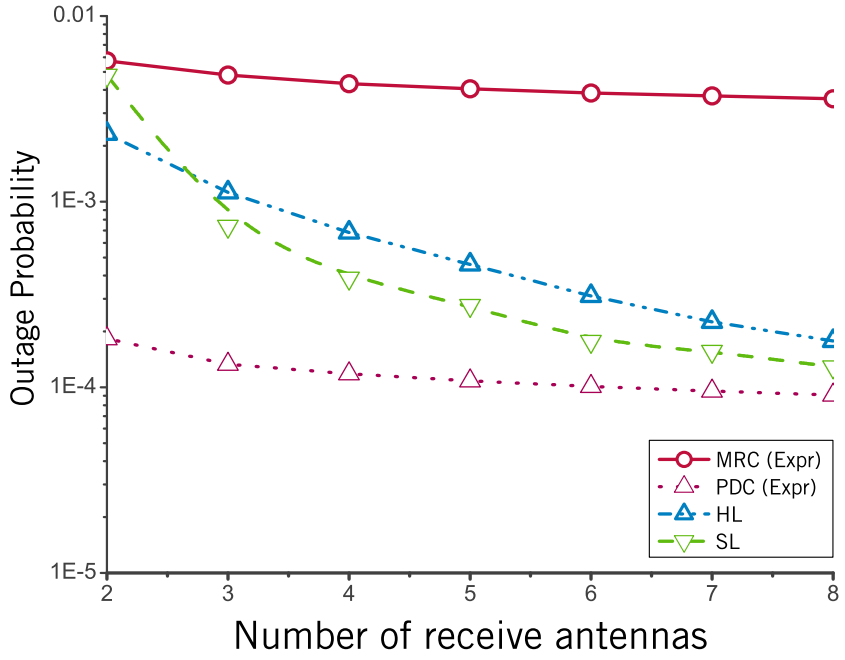

Fig. 9. Outage probability vs. number of receive antennas for maximal ratio combining (MRC), post-detection combining (PDC), and the novel hard-limiting (HL) and soft-limiting (SL) combiners in presence of partially spatially dependent interference. $\lambda_0 = 5 \times 10^{-5}, \lambda_e = 9.5 \times 10^{-4}$, $\tau = 1.0$, and $\eta = 2.0$ are used in simulations. Outage probability of MRC and PDC combining is evaluated using theoretical expressions.

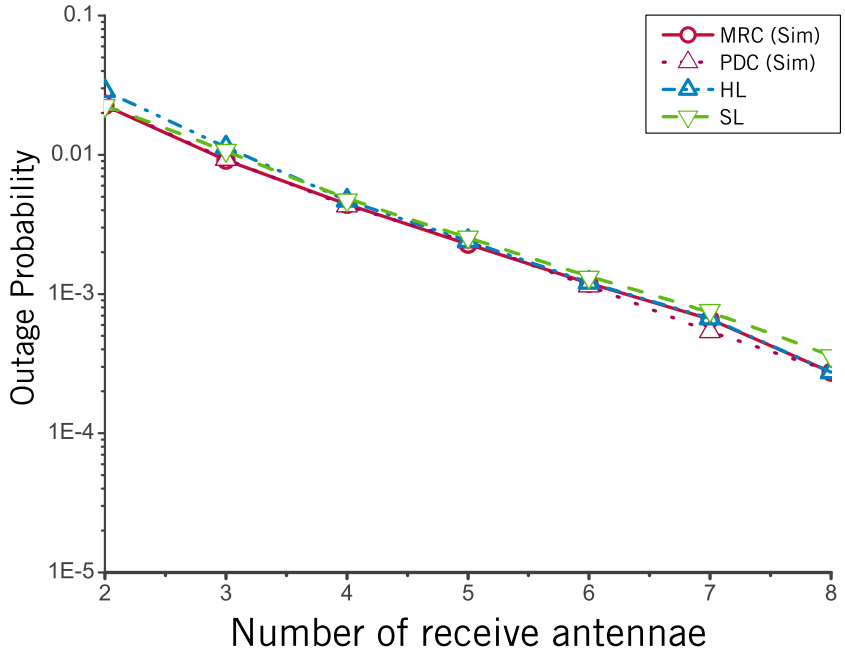

Fig. 10. Outage probability vs. number of receive antennas for maximal ratio combining (MRC), post-detection combining (PDC), and the novel hard-limiting (HL) and soft-limiting (SL) combiners in presence of Gaussian distributed interference. The variance of Gaussian interference is 0.05, $\tau = 1.0$, and $\eta = 2.0$. Outage probability of MRC and PDC combining is evaluated using numerical simulations.